Dewetting of Thin Amorphous Solid Water Films and Liquid-Cubic Ice Coexistence in Droplets Studied Using Infrared-Absorption and Secondary-Ion-Mass Spectroscopy

Ryutaro Souda*

Nanoscale Materials Center, National Institute for Materials Science, 1-1 Namiki, Tsukuba, Ibaraki 305-0044, Japan

Received: May 30, 2008; Revised Manuscript Received: July 25, 2008

The infrared absorption band of decoupled OD stretching vibration (4 mol% HOD in 20-monolayer H_2O) of amorphous solid water is red-shifted and sharpened at around 160 K because of spontaneous nucleation. The crystal grows in a fluidized liquid that forms droplets on a Ni(111) substrate. The shape change and red-shift of a coupled OH band during crystallization are elucidated by a Mie particle scattering model, indicating that nanometer-size droplets are formed preferentially. The spontaneous nucleation at 160 K is bypassed when amorphous solid water is deposited on a crystallized water film; the crystals grow around nuclei at ca. 150 K, resulting in larger crystal grains that do not cause Mie scattering. However, the crystal grains behave like viscous droplets because their morphology changes continuously after the completion of crystallization. The coexisting liquid-like water is indistinguishable from cubic ice in local structure. This behavior resembles that of a quasiliquid formed during premelting.

1. Introduction

The glass transition and crystallization of water is of importance for various research fields including astrophysics and cryobiology. Regarding the glass transition and crystallization temperatures of water, denoted respectively as T_g and T_c, widely different conclusions have been obtained from calorimetric studies.[1−5] Differential scanning calorimetry (DSC) indicates a very weak glass transition endotherm at 136 K before crystallization occurs at around 150 K.[4] We have used time-of-flight secondary ion mass spectrometry (TOF-SIMS) for the molecular-level analysis of the glass-liquid transition of amorphous solid water (ASW). Our results have revealed that water exhibits a very liquid-like nature at temperatures higher than T_g=136 K;[6−8] the self-diffusion of water molecules commences at 136 K and then the film dewets a Ni(111) surface after some aging time. The crystallization is most likely to occur in the liquid phase, but how liquid water evolves from ASW and crystallizes into ice Ic is still an open question. This paper clarifies the crystallization mechanism of thin ASW films and the nature of cubic ice by measuring spectra of reflection absorption infrared spectroscopy (RAIRS) and TOF-SIMS as a function of temperature. The crystallization of water has been discussed from the shape change in a stretching region of the IR absorption spectra.[9−15] We discuss how shape changes of a coupled OH band of H_2O and a decoupled OD band of HOD diluted in H_2O are related to the crystallization and film morphology from the comparison with the TOF-SIMS results.

It is believed that homogeneously crystallized water ice films can be grown by heating the ASW films deposited on transition-metal surfaces, such as Pt(111) and Ru(0001), to temperatures higher than ca. 150 K [16−18] because an ordered monolayer with structures that resemble those of a bilayer plane of crystalline ice is formed on these substrates.[19,20] The ASW film crystallization is thought to be promoted if ice I_c preexists on the surface; it is suggested that ice I_c grows homoepitaxially at temperatures well below T_g.[21,22] Recently, Kimmel et al. [23] have claimed nonwetting growth of fully crystallized water grains on Pt(111) and a hydrophobic character of the ordered water monolayer, but this phenomenon can be elucidated by the formation of viscous droplets as proposed by Jenniskens et al.[12] In this respect, Johari revealed the possibility of the water-cubic ice coexistence in nanometer-size droplets based on thermodynamic calculations of liquid−solid equilibrium.[24] However, the nature of cubic ice I_c, together with the amount of a coexisting amorphous phase, remains a subject of debate.[25] Here, we study thin ASW films deposited on the Ni(111) surface and crystallized water film and reveal a very liquid-like nature of water after crystallization.

2. Experimental Section

The TOF-SIMS experiment was performed in an ultrahigh-vacuum (UHV) chamber with a base pressure of less than 1×10^{-8} Pa. It was equipped with an electron-impact-type ion source and a linear TOF tube. The sample was floated with a bias voltage of +500 V; a pulsed He^+ beam (2.0 keV, ca. 10 pA/cm^2) was incident on the sample through a grounded stainless-steel mesh placed 4 mm above the sample surface. The secondary ions, extracted through the mesh, were detected using a channel electron multiplier. The substrate was the Ni(111) surface, which was cooled to 10 K using a closed-cycle helium refrigerator and heated to 1200 K by electron bombardment from behind. The cleanliness of the surface was checked in situ by TOF-SIMS; the contaminants assignable to hydrocarbons and K were visible just after insertion of the sample into the UHV chamber, but they were removed completely after several flash heatings. The H_2O molecules were adsorbed on the cleaned Ni(111) substrate by backfilling the UHV chamber. The coverage of the molecules was determined from the evolution curves of sputtered ion intensities as a function of exposure. One monolayer (1 ML) of the ASW film was attained by exposure of the H_2O molecules at around 2.5 L (1 langmuir (L) = 1.3×10^{-8} Pa·s). The TOF-SIMS spectra were recorded every 30 s at a ramping speed of 5 K min^{-1}.

* Corresponding author. E-mail: Souda.Ryutaro@nims.go.jp.

10.1021/jp8047828 CCC: $40.75
Published on Web 08/27/2008

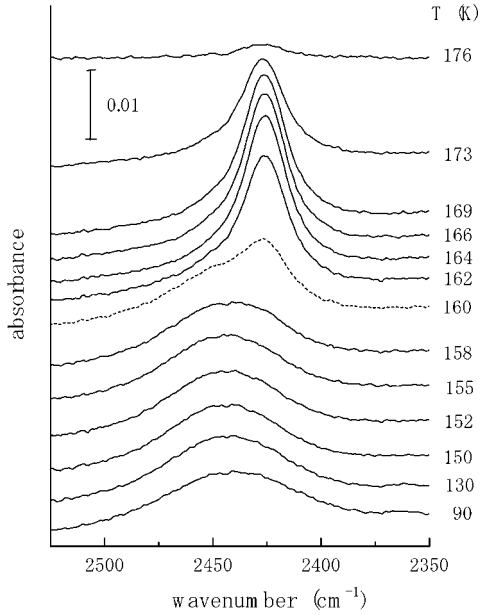

Figure 1. RAIR spectra of the OD stretching region for the HOD molecules (4 mol%) diluted in the H_2O matrix, as a function of temperature. The ASW film (20 ML) was deposited on the Au film at 90 K, and the temperature was ramped at a rate of 5 K min^{-1}.

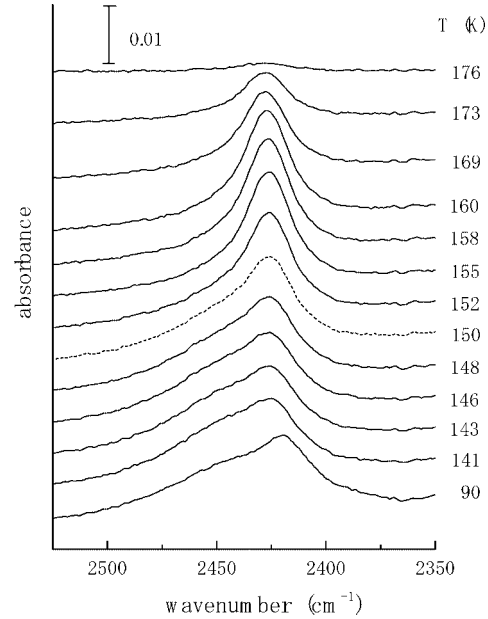

Figure 2. Changes in the RAIR spectra of the OD stretching band of the HOD molecules (4 mol%) as a function of temperature. The ASW film (20 ML) was deposited on the crystalline film (8 ML) that was formed by heating the ASW film to 160 K.

The RAIRS experiment was made in a separate UHV chamber with a base pressure of 3×10^{-8} Pa. The infrared absorption spectra were obtained using an FTIR spectrometer (FTS40A; Bio-Rad Laboratories, Inc.) equipped with a liquid-nitrogen-cooled mercury cadmium telluride detector. The IR beam was reflected from a gold film deposited on a mirror-finished Ni plate at a grazing angle. The substrate was cooled to 90 K using liquid nitrogen. The spectra were obtained over the wavenumber range of 400−4000 cm^{-1} with a 2 cm^{-1} resolution. The temperature was increased at the same ramping speed as that used for TOF-SIMS. The IR absorption band of the H_2O film consists of well separated stretching (3000−3700 cm^{-1}), bending (1500−1800 cm^{-1}), and libration (<1000 cm^{-1}) mode regions. The bending band was considerably broadened because of the overlapping with a libration overtone, similar to the FTIR spectra of crystalline and amorphous water.[26] Therefore, we focus on the stretching band regions that provide information about crystallization of the ASW film. The water films were deposited from the mixture of D_2O (2 mol%) in H_2O, thereby facilitating a study of the decoupled OD stretching band of HOD, together with the coupled OH stretching band of H_2O.

3. Results and Discussion

Figure 1 shows the OD stretching band for HOD in the 20 ML water film as a function of temperature. The band from the as-deposited ASW film exhibits a maximum at around 2443 cm^{-1}. The spectrum changes very little for temperatures of 90−158 K, at which the amorphous phase is dominant. The band narrows and shifts to 2425 cm^{-1} at temperatures higher than 160 K; the peak is asymmetric because a tail exists toward a low-frequency side. The red shift and sharpening of the spectra are caused by crystallization, corresponding to a more ordered environment. After crystallization, the peak shape is not changed until the water film evaporates at 176 K. This result indicates that homogeneous nucleation occurs abruptly at around 160 K. In the previous papers,[27,28] we have taken the RAIR spectra using the mixture of 5 mol% D_2O in H_2O, in which shoulders are recognizable more clearly for both lower and higher frequency sides of the narrow peak of crystals. We have suggested that the shoulders are caused by a coexisting amorphous phase. However, such shoulders are reduced considerably in the present result, indicating that they arise from coupling of the OD stretching vibration between the neighboring HOD molecules. Therefore, no direct evidence of the liquid-crystal coexistence is obtained solely from the IR absorption band shown in Figure 1.

We examined the manner in which crystal growth is affected by the preexisting nuclei. Figure 2 shows the decoupled OD stretching band of HOD from the ASW film (20 ML) deposited on the crystalline ice film that was formed by heating the ASW film (8 ML) to 160 K. The band initially consists of the overlapped crystalline and amorphous peaks: they change very little at temperatures less than 148 K. The intensity of the amorphous peak decreases at temperatures higher than 150 K because of crystallization of the ASW film. The spectrum is almost unchanged at temperatures higher than 155 K, at which temperature crystallization is thought to be completed. These results show clearly that crystallization is promoted by the preexisting nuclei.

The shape change in the coupled OH band has been discussed extensively for crystallization of ASW films.[12−14] Shown in Figure 3a is the OH stretching bands of the 20 ML ASW film before (146 K) and after (164 K) crystallization (the same RAIR spectra as in Figure 1). Three peaks are recognizable at around 3400, 3320, and 3170 cm^{-1} for the amorphous film. After crystallization occurs, the peak positions are red-shifted by ca. 50 cm^{-1} and their relative intensities change to a large extent. This behavior has been regarded as evidence of crystallization.[13,14] However, Figure 3b shows that the spectral change during crystallization is much less pronounced when the ASW film is deposited on ice I_c (as with RAIR spectra as in Figure 2); the red-shift value of the spectrum caused by crystallization (10−20 cm^{-1}) is smaller and the spectrum narrows slightly. Moreover, the intensity and position of the spectral peak depend on the film thickness as typically shown in Figure 4, which exhibits the OH stretching bands of the 200 ML water film deposited

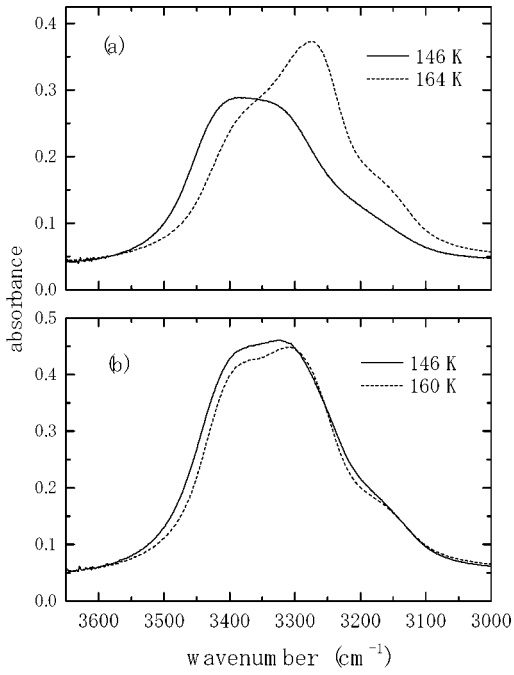

Figure 3. RAIR spectra of the coupled OH stretching band of the water molecules (20 ML) deposited on (a) the Au substrate and (b) the ice I_c film (8 ML). They are obtained from the same RAIR spectra as those for Figures 1 and 2.

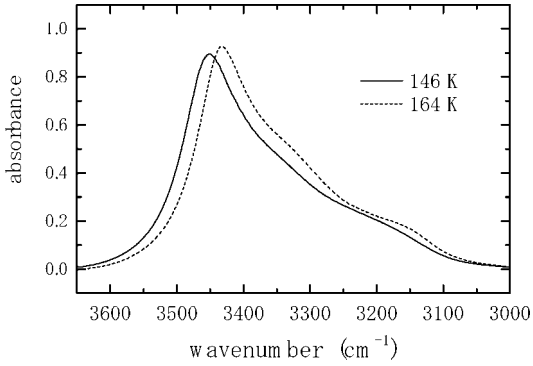

Figure 4. RAIR spectra of the coupled OH stretching band of the water film with a thickness of 200 ML.

on the Ni(111) surface. The main peak shifts to the higher wavenumber (3450 cm^{-1}) and increases in intensity, as compared to the peak in Figure 3a. The peak shift after crystallization (22 cm^{-1}) appears to be much smaller than that of the thinner film (50 cm^{-1}); it is closer to the value observed for the decoupled OD band, as depicted in Figure 1. Consequently, the drastic change in the positions and intensities of the peaks in Figure 3a cannot be attributed solely to crystallization.

More insights into the phase transition of water at around 160 K can be gained from the comparison between the TOF-SIMS and RAIRS results. Figure 5 shows the intensities of typical secondary ions from the H_2O (20 ML) adsorbed Ni(111) surface as a function of temperature. The $Ni^+(H_2O)$ ion is sputtered abruptly at around 160 K, where the H^+ intensity from H_2O drops. The Ni^+ and $Ni^+(H_2O)_n$ ions are created during collisions of sputtered Ni atoms with the H_2O molecules, as evidenced by the fact that their evolution curves are quite similar as a function of the H_2O coverage.[29] The probing depth of TOF-SIMS is 5−6 ML as far as the $Ni^+(H_2O)$ ion is concerned. Therefore, the dewetted film formed at around 162 K is thought to consist of droplets and thin layers of water without exposing the clean Ni(111) surface. The water crystallizes immediately

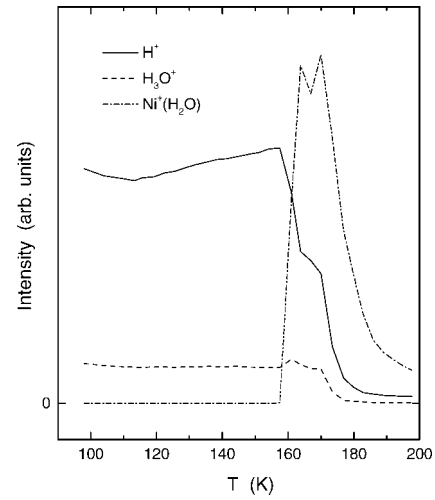

Figure 5. Temperature dependence of the TOF-SIMS intensities of typical secondary ions sputtered from the ASW film (20 ML H_2O) deposited on the Ni(111) substrate at 100 K. The temperature was increased at a rate of 5 K min^{-1}.

in droplets, thereby causing the simultaneous occurrence of dewetting (Figure 5) and crystallization (Figure 1) at around 160 K.

The TOF-SIMS result strongly suggests that the drastic change in the OH stretching band in Figure 3a is related not only to crystallization but also to film dewetting. In fact, the water film thicker than 80 ML does not dewet the Ni(111) substrate,[8] so that the spectral change in Figure 4 is much less pronounced than that in Figure 3a. It is well-known that the spectral shape and peak position in grazing-angle RAIRS of strongly absorbing media like water are largely influenced by the film thickness and morphology.[30] The RAIR spectra of nanometer-thick water films have been simulated using the Fresnel equation (for thin films) and Mie particle-scattering model.[31] The RAIR spectra before and after crystallization shown in Figure 3a are in good accord with the Fresnel and Mie spectra, respectively, simulated for polycrystalline water films in both shape and peak position. Therefore, the drastic shape change of the RAIR spectra can be explained by the formation of droplets rather than crystallization. On the other hand, the spectral feature of the crystalline film in Figure 3b (broken line) resembles that of the Fresnel spectrum simulated for the polycrystalline film with 0.5−20 nm thickness,[31] indicating that the formation of the Mie scatterer (nonometer-size droplets) is suppressed for the ASW film deposited on the crystalline ice surface. The same is true for the thicker film (Figure 4) which does not form droplets after crystallization. The spectral change observed for these films can be attributed to crystallization. In contrast to the OH band, the shape of the decoupled OD stretching band is independent of the film morphology and thickness (not shown).

Thin crystalline water films (<80 ML) are hardly grown without dewetting on the Ni(111) substrate. However, a uniformly wetted crystalline film is expected to be grown if the nuclei preexist on the substrate because the ASW film crystallizes at 150 K before dewetting occurs at 160 K. Figure 6 shows the TOF-SIMS intensities for the 20 ML ASW film deposited on the crystalline ice film (20 ML, forming droplets) as a function of temperature. It is noteworthy that the ASW film starts to dewet the Ni(111) substrate at around 150 K, simultaneously with the occurrence of crystallization. The film morphology changes continuously even after the crystallization

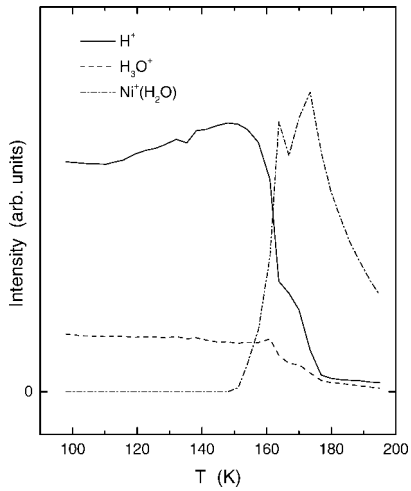

Figure 6. Temperature dependence of the TOF-SIMS intensities of secondary ions sputtered from the ASW film (20 ML H_2O) deposited on the crystalline ice film at 100 K. The crystalline film was prepared by heating the ASW film (20 ML) to 160 K.

is completed at 155 K, as revealed from the continuous evolution of the $Ni^+(H_2O)$ intensity. The increase in the $Ni^+(H_2O)$ yield has nothing to do with the evaporation of the film with increasing temperature because film dewetting is observed for isothermal TOF-SIMS measurements at 150 K (not shown). The overall behavior of the secondary ion intensities is fundamentally identical to that shown in Figure 5, but the morphology of the crystalline film in Figures 6 must be different from that in Figure 5, as evidenced by the different evolutions of the secondary ions. The crystal grains thus formed via "homoepitaxial growth" are vastly different from ordinary crystals characterized by a high rigidity and have a strong resemblance to a viscous liquid.

The evolution of a liquid phase is prerequisite for crystallization of water. In the previous papers, we have revealed that liquid-like water is formed in two steps.[6−8] A distinct liquid (low density liquid: LDL) is formed at the conventional glass transition temperature (T_g = 136 K). LDL is characterized by translational molecular diffusivity without apparent fluidity. The short-range order of LDL is same as that of ASW, as evidenced by the invariance of the IR absorption band at this temperature as seen in Figure 1. A fluidized liquid causing film dewetting is formed after some aging time, which is observed at around 160 K in the temperature-programmed TOF-SIMS experiments. This phenomenon can be interpreted as the formation of supercooled liquid water (SLW) because of the following reasons. The spontaneous nucleation is a characteristic of SLW that is unstable below 235 K. An aqueous LiCl solution is formed from the ASW-adsorbed LiCl film at ca. 160 K,[8,27] which can be explained as dissolution of LiCl into SLW. Moreover, hydrophobic species that are incorporated from the surface into the bulk of the ASW film are dehydrated almost completely before dewetting occurs,[7,8] perhaps partly because of their poor solubility in SLW. An unusually small specific heat jump observed in DSC at T_g = 136 K[4] is thought to be attributable to the glass-liquid transition of distinct water (ASW→LDL), whereas the endotherm expected for the liquid−liquid phase transition (LDL→SLW) at around 160 K might be hindered by the huge crystallization exotherm. Thus, LDL can be classified as a "strong" liquid, although SLW is expected to be a "fragile" liquid that exhibits a very sharp change in heat capacity.[32]

The phase transition (or spontaneous nucleation) of water is bypassed when ASW is deposited on the crystalline ice film; the crystal grows around the nuclei in LDL, thereby forming greater crystal grains. However, the crystal grains exhibit viscous nature as evidenced by the continuous change in the film morphology. The RAIRS study revealed that methanol lowers the crystallization temperature of ASW to 150 K,[28] as did the crystalline nuclei observed in this study, whereas film dewetting is quenched up to the evaporation temperature (170−180 K) because surface tension is relaxed by methanol.[6,28] The surfactant effect evidences the roles of the surface tension of the fluidized liquid in film dewetting, rather than the bulk-initiated crystallization. Thus, the liquid-like property of water after crystallization is manifested.

The present result is consistent with the observation using transmission electron microscopy: Jenniskens et al.[12] reported that the viscous droplets are formed during crystallization of the ASW film to ice I_c at temperatures of 140−220 K. Crystallization is inhibited when only 30% has transformed; most of the ice persists as a viscous liquid prior to its crystallization to ice I_h. The thermodynamic basis for this observation is provided by Johari[24] who showed that the melting temperature is lowered with decrease in radius of cubic ice particles. This result might also explain the infrared absorption spectra of quenched aerosols, which are characterized as having a cubic ice core and disordered surface and subsurface regions.[15] The situation is the same in the present case because crystallization occurs in the nanometer-size droplets formed on the Ni(111) substrate. On the other hand, a liquid-like property is observed for a thick crystalline film (200 ML) as well, as evidenced by the incorporation of a monolayer of NaCl into the film at temperatures higher than 150 K.[33] The coexistence of amorphous phase with ice I_c has been suggested by DSC and X-ray diffraction study of hyperquenched glassy water (HGW), but at most 20% amorphous component is included in the crystallized film[25] in contrast to the result of Jenniskens et al.[12] The discrepancy might be explained by different qualities between the HGW and ASW films. The HGW film (1.5 mm in thickness), which is prepared by vitrification of aqueous aerosol droplets (5 μm in diameter), contains at least 5−30% crystalline ice I_c, depending on the cooling speed.[34,35] Therefore, the growth of such nuclei results in a larger crystal grains than those formed by spontaneous nucleation in the ASW film, as verified in the present study. The liquid-like phase exists on the surface or grain boundaries, so that the amorphous component is smaller for the larger grains formed via crystallization of HGW. The melting-layer thickness can be estimated from the result of a temperature programmed desorption study:[36] a complete mixing of hydrogen isotopes occurs in binary ASW films (D_2O/ H_2O) over the entire length of 66 ML (approximately 20 nm), although the ASW film of this thickness forms droplets. Consequently, the controversies regarding the amorphous component between electron and X-ray diffraction studies are attributable to the difference in the crystal grain size and initial film thickness.

Despite the liquid-cubic ice coexistence, the RAIR spectra in Figures 1 and 2 show a single peak after crystallization although a tail extends toward the higher wavenumber side. The occurrence of liquid water is identifiable by the evolutions not only of the blue-shifted and broadened stretching band but also of the intense bending band, but no indications of the coexisting liquid water are obtained at all in the present study. This result indicates that the structure of liquid-like water coexisting with crystallites is largely different from that of normal liquid water. The surface or intergranular melting at temperatures below the bulk melting point (T_m) is a well-known phenomenon.[37−40] Therefore, the liquid-ice I_c coexistence might be elucidated using

the idea of premelting. The premelting manifests itself in gradual disordering of the surface region and the occurrence of self-diffusion at temperatures below T_m; the surface melted layer is sometimes called a "quasiliquid" layer because its property is different from that of bulk liquid. In fact, quasiliquid persists both short-range order of crystals and liquid-like mobility,[38,39] so that it can be regarded as a strongly correlated liquid or a lattice fluid. Therefore, it is very likely that the quasiliquid layer is also formed on the surface of ice I_c in the deeply supercooled region. The quasiliquid layer might not be distinguishable from the ice I_c grain based on the IR absorption spectra because of the short-range order resemblance to the crystal; therefore, its presence must be checked by the microscopic transport properties of molecules or the macroscopic fluidity of the film as discussed in the present study. The quasiliquid layer might play a role in the progressive transformation of ice I_c to ice I_h at higher temperatures, although ice I_c is predominant in the 160−220 K range.[41] This behavior might explain the instability of vapor-deposited ice films that are formed on the surface of $BaF_2(111)$ at 208 K.[42]

4. Conclusion

The decoupled OD stretching band of the HOD molecules diluted in the amorphous H_2O film exhibited a red shift and sharpening at temperatures higher than 160 K because of crystallization. On the other hand, the identification of crystallization using the coupled OH band is not straightforward because the peak position, shape, and intensity are strongly dependent on the film thickness and morphology. The large red-shift value (50 cm^{-1}) of the peaks observed at 160 K cannot be attributed solely to crystallization. The spectral change is rather explainable by the Mie scattering from nanometer-size droplets. The Mie scattering contribution decreases considerably for the ASW film deposited on the crystalline film because larger crystals grow around the nuclei at 150 K before spontaneous nucleation occurs. The crystal grains thus formed coexist with the liquid-like phase, as evidenced by the continuous change in film morphology after crystallization, but the IR band shows no evidence of a coexisting amorphous phase. The liquid-like phase observed here might have the same property of quasiliquid formed during premelting of ice I_h; both of them are expected to have short-range-order similarity to the crystalline ice. Thus, three distinct forms of liquid water might exist, i.e., low density liquid, normal and supercooled water, and quasiliquid coexisting with cubic ice.

References and Notes

(1) Mcmillian, J. A.; Los, S. C. *Nature (London)* **1965**, *206*, 806.
(2) Ghormley, J. A. *J. Chem. Phys.* **1967**, *48*, 503.
(3) McaFarlane, D. R.; Angell, C. A. *J. Phys. Chem.* **1984**, *88*, 759.
(4) Johari, G. P.; Hallbrucker, A.; Mayer, E. *Nature* **1987**, *330*, 552.
(5) Velikov, V.; Borick, S.; Angell, C. A. *Science* **2001**, *294*, 2335.
(6) Souda, R. *Phys. Rev. Lett.* **2004**, *93*, 235502.
(7) Souda, R. *J. Chem. Phys.* **2004**, *121*, 8676.
(8) Souda, R. *J. Chem. Phys.* **2006**, *125*, 181103.
(9) Hage, W.; Hallbrucker, A.; Mayer, E.; Johari, G. P. *J. Chem. Phys.* **1994**, *100*, 2743.
(10) Hage, W.; Hallbrucker, A.; Mayer, E.; Johari, G. P. *J. Chem. Phys.* **1995**, *103*, 545.
(11) Delzeit, L.; Devlin, J. P.; Buch, V. *J. Chem. Phys.* **1997**, *107*, 3726.
(12) Jenniskens, P.; Banham, S. F.; Blake, D. F.; McCoustra, M. R. *J. Chem. Phys.* **1997**, *107*, 1232.
(13) Backus, E. H. G.; Grecea, M. L.; Kleyn, A. W.; Bonn, M. *Phys. Rev. Lett.* **2004**, *92*, 236101.
(14) Ostblom, M.; Ekeroth, J.; Konradsson, P.; Liedberg, B. *J. Phys. Chem. B* **2006**, *110*, 1695.
(15) Devlin, J. P.; Joyce, C.; Buch, V. *J. Phys. Chem. A* **2000**, *104*, 1974.
(16) Smith, R. S.; Huang, C.; Wong, E. K. L.; Kay, B. D. *Phys. Rev. Lett.* **1997**, *79*, 909.
(17) Smith, R. S.; Kay, B. D. *Nature (London)* **1999**, *398*, 788.
(18) Cowin, J. P.; Tsekouras, A. A.; Iedema, M. J.; Wu, K.; Ellison, G. B. *Nature (London)* **1999**, *398*, 405.
(19) Thiel, P. A.; Madey, T. E. *Surf. Sci. Rep.* **1987**, *7*, 211.
(20) Henderson, M. A. *Surf. Sci. Rep.* **2002**, *46*, 1.
(21) Dohnalek, Z.; Ciolli, R. L.; Kimmel, G. A.; Stevenson, K. P.; Smith, R. S.; Kay, B. D. *J. Chem. Phys.* **1999**, *110*, 5489.
(22) Lofgren, P.; Ahlstrom, P.; Chakarov, D. V.; Lausmaa, J.; Kasemo, B. *Surf. Sci.* **1996**, *367*, L19.
(23) Kimmel, G. A.; Petrik, N. G.; Dohnalek, Z.; Kay, B. D. *Phys. Rev. Lett.* **2005**, *95*, 166102.
(24) Johari, G. P. *J. Chem. Phys.* **1998**, *109*, 1070.
(25) Kohl, I.; Mayer, E.; Hallbrucker, A. *Phys. Chem. Chem. Phys.* **2000**, *2*, 1579.
(26) Devlin, J. P.; Sadlej, J.; Buch, V. *J. Phys. Chem. A* **2001**, *105*, 974.
(27) Souda, R. *J. Phys. Chem. B* **2007**, *111*, 6528.
(28) Souda, R. *Phys. Rev. B* **2007**, *75*, 184116.
(29) Souda, R. *Phys. Rev. B* **2004**, *70*, 165412.
(30) Greenler, R. G. *J. Chem. Phys.* **1966**, *44*, 310.
(31) Mitlin, S.; Leung, K. T. *J. Phys. Chem. B* **2002**, *106*, 6234.
(32) Angell, C. A. *Science* **2008**, *319*, 582.
(33) Souda, R. *J. Phys. Chem. B* **2007**, *111*, 11209.
(34) Tulk, C. A.; Klug, D. D.; Branderhorst, R.; Sharpe, P.; Ripmeester, J. A. *J. Chem. Phys.* **1998**, *109*, 8478.
(35) Hallbrucker, A.; Mayer, E. *J. Phys. Chem.* **1987**, *91*, 503.
(36) Smith, R. S.; Huang, C.; Kay, B. D. *J. Phys. Chem. B* **1997**, *101*, 6123.
(37) Frenken, J. W. M.; van der Veen, J. F. *Phys. Rev. Lett.* **1985**, *54*, 134.
(38) Bienfait, M.; Gay, J. M.; Blank, H. *Surf. Sci.* **1988**, *204*, 331.
(39) Maruyama, M.; Bienfait, M.; Liu, F. C.; Liu, Y. M.; Vilches, O. E.; Rieutord, F. *Surf. Sci.* **1993**, *283*, 333.
(40) Ishizaki, T.; Maruyama, M.; Furukawa, Y.; Dash, J. G. *J. Cryst. Growth* **1996**, *163*, 455.
(41) Johari, G. P. *J. Chem. Phys.* **2005**, *122*, 194504.
(42) Sadtchenko, V.; Ewig, G. E. *Langmuir* **2002**, *18*, 4632.

JP8047828